Imaging Simulations including Pointing Error for Single Pointing Observations: Prelimiary Results

Koh-Ichiro Morita

May 18th 2000

ABSTRACT

Several imaging simulations for single pointing observations have been conducted including pointing error. Array configurations used in these simulations are a ring array and a spiral array. A multi-compact-Gaussian model was used as a source model. In the case of no pointing error, results shows that we can obtain very high quality images with both array configurations and there is a significant difference of image qualities depending on array configuraions and hour angle ranges. However, when we added some pointing errors to the simulated data, the image quality was reduced dramatically and the large difference of image quality disappears. For example, dynamic ranges of no pointing error cases are from 4,000 to 15,000 but from 2,000 to 3,000 for 1 arcsec pointing error and around 1,000 for 2.5 arcsec pointing error at 230 GHz.

---

1. Introduction

In order to select the optimum array configuration, the ALMA configuration working group have conducted extensive simulation campaigns. Basic strategy of the simulations are to test the imaging quality of the configurations using several standard images. However, in current plan, these simulations would be performed without any errors added to the simulated data. From previous configuration studies (e.g. Morita, 1996), error-free imaging simulations with the trial configuration sets are expected to produce dynamic ranges on the order of 10,000:1 or greater.

Cornwell et al. (A. & Ap. 1993) showed that pointing errors will likely limit the dynamic range of mosaiced images at millimeter wavelengths. Current specification of pointing accuracy for 12 m antenna of the ALMA is about 0.6 arcsec. It is about

5 % of FWHM at 350 GHz and Holdaway (MMA Memo 61, 1990) demonstrated that this pointing error will limit the dynamic range about 500-1000:1. We should also expect that such a degradation of image quality will appear even in single pointing observations.

Since the degradation caused by the pointing error is very large, the result of evaluation of array configurations including the pointing errors could be very different from that without errors. To see the difference, we have conducted the imaging simulations including the pointing errors. In these simulations we used two extreme types of array configurations, a ring array that makes uniform (u,v) distribution and a spiral array that makes tapered (u,v) distribution. In this short memo, we show preliminary results of the simulations.

2. Imaging Simulations

2.1 Limitation of Imaging Simulation

To generate visilibity include the antenna pointing errors is a time consuming task. We need a Fourier transform to calculate each visiblity at every integration. For example, the case of 1k x 1k model image and 64 antennas, the calculation for an integration takes about 1 hour with Ultra SPARCII 400 MHz with 2 GByte memory. Therefore, we limited the input image size to 256 x 256.

In the case of a ring array for 64 12 m antennas, the minimum array diameter is about 312m because the minimum spacing is 1.3 times the antenna diameter. Since we need to make some randomization for better imaging performance, we set the array diameter for the ring array is 420 m. The FWHM of the corresponding synthesized beam (/Delta/theta) is about 0.44 arcsec at 230 GHz. Because field of view for imaging should be larger than the FWHM (~ 22 arcsec at 230 GHz) of the primary beam pattern, the cellsize was set to be 0.12 arcsec. In this case, the field of view is about 31 arcsec. The cellsize is ~ 35 % larger than 0.2 x /Delta/theta which is a recommendation of the configuration working group.

2.2 Array Configurations

For a ring array, we located 64 antennas randomly along the ring with a diameter of 420 m. The configuration of the ring array is shown in Figure 1 (a).

To generate a spiral array which has similar resolution to the ring array, we reduced and modified an array configuration originarly proposed by J. Conway. The diameter of the array is about 750 m. The array configuration is shown in Figure 1 (b).

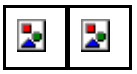

(a) (b)

Figure 1. Array configurations of test arrays used in the imaging simulations. (a) A spiral array with a diameter of 750 m. (b) A ring array with a diameter of 420 m

2.3 Source Models

A multi-compact-Gaussian model was used for input image to the simulation. We generated 30 compact elliptical Gaussians of which rms FWHM is about 0.5 arcsec in the area with a diameter of about 27 arcsec. We set the area for distribution of the components larger than the FWHM of the primary beam a little, because source sizes are often comparable to the primary beam size in observations at millimeter wavelengths with existing 10 - 15 m antennas. Figure 2 shows the image model.

Figure 2. The source model used in the imaging simulations.

2.4 Visibility Generation

We have used SDE package to simulate visibility with the pointing error. Our model for antenna pointing errors is same as that of Cornwell et al. (1993), which consists of following four terms: a global pointing offset, an initial pointing offset, a dirft, and a random component. We multiplied the input image by the primary beam pattern with the pointing error and obtained each visibility by a direct Fourier transform. Number of direct Fourier transforms needed to generate a simulation data is equal to the number of visibilities. To calculate visibilities from a 256 x 256 image for every integration takes about 3 minutes with Ultra SPARCII 400 MHz.

2.5 Data Reduction

The data reduction has been done with the classic AIPS package. We used the UNIFORM weight for the gridding and MX CLEAN for deconvolution.

2.6 Other Simulation Parameters

Table 1.

Source Decl.	**-30.0 deg**

Integration Time	60 sec.
Hour Angle Range (hour)	[0, 0.2], [0, 1]
Observing Frequency	230 GHz

3. Results

3.1 (u,v) Coverage and Beam Pattern

Figure 3 shows a (u,v) coverage and a radial profile of (u,v) sampling density for the spiral array with an hour angle range of [0, 1] hour. The radial profile clearly shows the tapered spatial filering characteristics of the (u,v) coverage. Correponding synthesized beam pattern is shown in Fig. 5.

A (u,v) coverage and a radial profile of (u,v) sampling density for the ring array with an hour angle range of [0, 1] hour are shown in Figure 4. The radial profile shows fairly uniform filtering characteristics with a central dense part. A dotted line in Figure 5 shows the corresponding synthesized beam.

Table 2 shows levels of near and far sidelobe. Radial range of near sidelobe region was defined from 1 x /Delta/theta to 10 x /Delta/theta.

Table 2.

Array	HA coverage (hour)	Near sidelobe PEAK	Near sidelobe RMS (%)	Far sidelobe PEAK	Far sidelobe RMS (%)
SPIRAL	[0, 0.2]	6.6	1.3	12.0	1.4
RING	[0, 0.2]	17.2	2.9	9.9	1.1
SPIRAL	[0, 1]	10.9	1.2	4.1	0.7
RING	[0, 1]	19.3	2.4	3.9	0.5

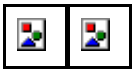

Figure 3. The (u,v) coverage and the (u,v) radial profile for the spiral array.

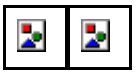

Figure 4 The (u,v) coverage and the (u,v) radial profile for the ring array .

Figure 5. Synthesized beams. A solid line is for the spiral array and a dotted line is for the ring array. Hour angle range is [0, 1.0] hour.

3.2 Imaging Quality

In Figure 6, we show a result of the imaging simulation using the spiral array for an hour angle range of [0.0, 1.0] hour with no pointing error. Figure 6 (a) and (b) are a deconvolution image and a residual from the model image convoleved with the CLEAN beam, respectively. This result clearly shows that imaging error distribution is not uniform and maginitudes of imaging errors in on-source area and off-source area are quite different from each other. Therefore, we evaluated image quality using the dynamic range (off-source error) and the median fidelity index (on-source error) (Cornwell et al, 1993). For the on-source area, we picked up the area larger than 0.1 % of the peak of the model image. In the case of Figure 6, the dynamic range is about 14,300 and the fidelity index is 103.

Residual images for the spiral array and the ring array with the rms pointing error of about 0.51 arcsec are shown in Figure 7 (a) (b), respectively. The hour angle range is also [0, 1] hour. In these cases, the dynamic ranges are 4,770 and 3,680 for the spiral and the ring, respectively. The image fidelities are 34.3 and 24.4.

In Figure 8 we plotted the dynamic ranges for various combinations of array configurations and hour angle ranges as a function of the rms pointing error. A similar plot for the fidelity indexes are shown in Figure 9. These figures clearly show that even small rms pointing errors (less than 0.5 arcsec) affect resultant image quiality very much. The dynamic range and the fidelity index with 0.5 arcsec pointing error, are less than half of those without the pointing error. There are siginificant difference between image qualities without the pointing error, which probably depend on the array configurations and the hour angle range. However, no such large differences are seen in the results with the pointing errors.

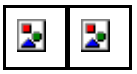

(a) (b)

Figure 6. Results of the imaging simulations using the spiral array for HA coverage of [0.0, 1.0] hour and no pointing error. (a) is a deconvolution image and contours are [-1, -0.5, -0.2, -0.1, 0.1, 0.2, 0.5, 1, 2, 5, 10, 20, 50] % of the peak. (b) is a residual image and contours are [-10, -5, -2, -0.5, -0.2, -0.1, -0.05, 0.05, 0.1, 0.2, 0.5, 1, 2, 5, 10] % of the peak.

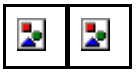

(a) (b)

Figure 7. Residual images for the spiral array and the ring array. The rms pointintg error is about 0.51 arcsec and the hour angel range is [0, 1] hour. Contours are same as in Figure 6 (b).

Figure 8. The dynamic ranges vs the pointing errors.

Figure 9. The fidelity indexes.

4. Discussion

Our preliminary results indicate that the pointing error could affect the evaluation of array configurations very much. The model which was used these simulations consists of many compact components distributed in the area which is almost comparable to primary beam width. The image degradation due to the pointing error depends on source size and the results probably show the worst case. However, from experiences of observations with existing 10 - 15 m antennas at millimeter wavelengths, we should expect that a lot of objects for the ALMA are comparable to or larger than the primary beam size.

Current problem of the imaging simulation including the pointing error is computing time. Even if we limit the image size to 256 x 256, we need more than 10 hours for full synthesis observations. For sparse configurations, 1024 x 1024 image size should be desired but it is hard to conduct such simulations by the current programs. To

evaluate various array configurations with the pointing errors, we need more effective program to generate visibilities with the pointing error.

References

Cornwell, T. J., Holdaway, M. A., and Uson, J. M., 1993, " Radio-interferometric Imaging of Very Large Objects: Implication for Array Design", A. & Ap. 271, 697-713.

Holdaway, M. A., 1990, MMA memo 61, "Imaging Characteristics of a Homogeneous Millimeter Array".

Morita, K.-I., Ishiguro, M. and Holdaway, M. A., 1996, URSI-GA, "Array Configuration of the Large Millimeter and Submillimeter Array (LMSA)".